Extracting accurate strain measurements in bone mechanics: A critical review of current methods

Grassi, Lorenzo; Isaksson, Hanna

Published in:
Journal of the Mechanical Behavior of Biomedical Materials

DOI:
10.1016/j.jmbbm.2015.06.006

2015

www.elsevier.com/locate/jmbbm

Extracting accurate strain measurements in bone mechanics: A critical review of current methods

Lorenzo Grassi, Hanna Isaksson

PII: S1751-6161(15)00198-8
DOI: http://dx.doi.org/10.1016/j.jmbbm.2015.06.006
Reference: JMBBM1499

To appear in: *Journal of the Mechanical Behavior of Biomedical Materials*

Received date: 8 January 2015
Revised date: 1 June 2015
Accepted date:
2 June 2015

Cite this article as: Lorenzo Grassi, Hanna Isaksson, Extracting accurate strain measurements in bone mechanics: A critical review of current methods, *Journal of the Mechanical Behavior of Biomedical Materials,* http://dx.doi.org/10.1016/j.jmbbm.2015.06.006

Lorenzo Grassi [1], and Hanna Isaksson [1]

1. Department of Biomedical Engineering, and Department of Orthopedics, Lund University, Lund, Sweden

EXTRACTING ACCURATE STRAIN MEASUREMENTS IN BONE MECHANICS: A CRITICAL REVIEW OF CURRENT METHODS.

CORRESPONDING AUTHOR:
Lorenzo Grassi, M.Sc.
Department of Biomedical Engineering, Lund University, P.O. Box 118, SE-221 00, Lund, Sweden
lorenzo.grassi@bme.lth.se
+46 (0) 46 222 0655

Abstract

Osteoporosis related fractures are a social burden that advocates for more accurate fracture prediction methods. Mechanistic methods, e.g. finite element models, have been proposed as a tool to better predict bone mechanical behaviour and strength. However, there is little consensus about the optimal constitutive law to describe bone as a material. Extracting reliable and relevant strain data from experimental tests is of fundamental importance to better understand bone mechanical properties, and to validate numerical models.

Several techniques have been used to measure strain in experimental mechanics, with substantial differences in terms of accuracy, precision, time- and length-scale. Each technique presents upsides and downsides that must be carefully evaluated when designing the experiment. Moreover, additional complexities are often encountered when applying such strain measurement techniques to bone, due to its complex composite structure.

This review of literature examined the four most commonly adopted methods for strain measurements (strain gauges, fibre Bragg grating sensors, digital image correlation, and digital volume correlation), with a focus on studies with bone as a substrate material, at the organ and tissue level. For each of them the working principles, a summary of the main applications to bone mechanics at the organ- and tissue-level, and a list of pros and cons are provided.

Keywords

Strain, bone mechanics, femur, validation, strain gauges, strain gages, fibre Bragg grating, digital image correlation, digital volume correlation.

1. Introduction

Understanding bone mechanical behaviour under different loading conditions is of great importance to prevent and treat bone fracture in individuals. Finite element (FE) models have been proposed as an automatic and mechanistic method to assess bone strength and fracture risk in individuals [1]–[3]. However, there is no consensus about the optimal constitutive model and bone strength criterion to be implemented in such FE models [4]–[7]. This is because bone is a complex composite material, with properties that among other things change with time- and length-scale [8], [9]. Treating bone fractures, e.g. in the form of total joint replacement or a fixation device, requires knowledge of the mechanical stimuli exerted by such devices, since bone can remodel itself in response to the local mechanical stimulation [10], [11]. FE models can also help predicting the outcome of such surgical treatments if bone mechanical properties and strength are correctly modelled.

To identify the optimal material model for bone and account for the intrinsic inter- and intra-patient variability, the design of proper experiments with the aim of 1) better characterizing bone material properties, and 2) providing a validation benchmark for numerical investigations [12]–[14] is required. Depending on the specific aim, such experimental tests can be performed at different time- and length-scales. However, all the experiments need to extract reliable quantitative information about bone behaviour. Apart from recording the overall force and displacement during the experiment, usually displacements and strains can be measured at different locations over the tested samples. Depending on the required time, spatial resolution and the kind of mechanical tests performed, several techniques can be used to measure bone strain.

The continuous technological development provides new measurement tools with increased accuracy and precision. Consequently, the obtained strain data increases both in resolution and number, from the first discrete measurements using extensometers, to the full-field reconstructions achieved today with optical methods. The technological development, however, does not guard against instrumentation misuse, and/or data misinterpretation. Methodological studies are available for each of the different strain measurement techniques [15]–[18]. Nevertheless, a vast majority of those was performed using flat, polished, and standardized specimens of polymeric or metallic materials. Human bones present additional complexities when it comes to strain measurements,

mainly due to the geometry, surface roughness and humidity. As a consequence, additional care needs to be taken when measuring strains in human bones.

To our knowledge, an extensive review that covers the principal techniques for strain measurement with focus on human bone is lacking in the literature. Earlier reviews are either outdated and does therefore not include the latest developments [19]–[22], or limited to one single strain measurement technique [23]. Our aim is to provide a comprehensive review of the most commonly adopted methods to measure strains on bone, at a length scale of the organ- and tissue-level. The main methods of strain measurement adopted in bone biomechanics are reviewed, with their main applications, as well as their pros and cons. It is our intention that this manuscript should act as a reference guide for researchers who are designing a new experiment and need to choose the most suitable strain measurement method.

2. Approach

A first literature search was performed to identify the most relevant techniques for strain measurements on bone at the organ level. A review of some of the most relevant books on experimental biomechanics of bone [24], [25] was made together with the analysis of the results of a "(strain OR measurement) AND bone" PubMed (http://www.ncbi.nlm.nih.gov/pubmed/) search. Four strain measurement techniques were identified (Figure 1), as they were most frequently used in the spanned range of literature:

- Strain gauges
- Fibre Bragg grating sensors
- Digital image correlation
- Digital volume correlation

For each of the methods, a brief description of the principles, followed by a summary of the most relevant applications to bone biomechanics is provided. The cited studies were retrieved through a PubMed search, focusing on the applications of each technique on human bone samples at the organ-level length scale (Table 1). Where many studies on human bones were available, priority was given to studies of the femur due to its high fracture incidence [26]. A few studies investigating the micro-scale behaviour of bone were included for digital volume correlation, since the state-of-the-art studies with this technique were performed based on micro-CT data.

2.1 Strain gauges

The first application of bonded strain gauges (SG) was reported in 1938, and the first application to bone biomechanics dates only a few years later [27]. Since then, SGs have been heavily used in bone biomechanics, and they are still considered the gold standard in bone strain measurement because of their accuracy and high frequency response.

2.1.1 Working principles. SGs measure the strains by reading the increase/decrease of the resistance of a metallic material when exposed to an external tensile/compressive force that elongates/contracts it. Given the original resistance of the material, R, its variation as a function of the applied strain, ε, is given by: $\Delta R / R = K_s \epsilon$, where K_s is the gauge factor, the coefficient expressing the SG sensitivity [28]. A backing material carries deformation from the tested material to the electrical grid. SG typically have 3 differently oriented gauge grids (Figure 1a). This so called "rosette" configuration allows to obtain 3 independent strain measurements in different directions, and thus determine the principal strains and principal strain orientations. An accurate strain measurement requires a proper bonding of the backing material to the specimen. Optimally, the

surface for SG measurement should be chemically clean, with an appropriate roughness, a surface alkalinity corresponding to a pH of 7, and a visible gauge layout lines for locating and orienting the SG [29]. Bone does not have these features, and therefore different procedures have been adopted to optimize the bone surface for SG applications.

2.1.2 Most relevant studies. From the PubMed search, 239 publications were retrieved, where of four were considered most relevant. One additional study from a journal not indexed in PubMed [30] was also reported (Table 1). Roberts [30] defined a set of procedures to apply SGs on bone samples. These procedures included wiring, bonding, and waterproofing. The bone surface was prepared by removing all soft tissue and subsequently degreasing it with acetone, while body fluids were absorbed using sponges. SGs were bonded using cyanoacrylate or epoxy resins. Waterproofing was performed by coating the gauge top surface and wiring junctions with Glyptol and silicon rubber, whereas Teflon-insulated copper was used for wiring. As will be shown below, only minor modifications to this protocol have been introduced in the following 50 years.

Kim et al. [31] investigated the strain distribution in the proximal human femur using SGs in response to the insertion of two different types of femoral stems. Ten 45^{o} rosettes (3x1.25 mm rectangular grid, 9x9 mm measuring grid carrier) were bonded to the proximal femora at four levels, namely at the calcar (medial side) and 2, 4, and 8 cm distal to the most caudal part of the femoral head. Bone surface was prepared for strain measurement by sandpapering, degreasing with acetone and drying in O_2 stream. An etchant was applied to the gauge site, and then rinsed with saline. SGs were bonded with two-component PMMA adhesive, and waterproofed using epoxy sealing. Femora were first tested in the intact configuration (900 N for all specimens), and then after the stem components insertion. A study adopting an almost identical procedure was proposed by Aamodt et al. [32]. Also, the same specimen preparation and strain gauge application procedure was adopted recently to investigate the different mechanical response of composite and cadaver femora [33].

A few years later, Ostbyhaug et al. [34] investigated the cortical strain pattern in response to insertion of two types of femoral stems. Twelve pairs of contralateral femora were obtained, and the stem was implanted randomly in the left or right femur. On each specimen, ten strain-gauge rosettes (3x1.25 mm rectangular grid, 9x9 mm measuring grid carrier) were attached at four levels at the medial, lateral, and anterior aspects of the proximal femur. The bone surface was prepared for strain measurement by using acetone and etchant. The SGs were bonded using two-component PMMA adhesive, and subsequently waterproofed using a sealant.

In the same years, the group of Cristofolini & Viceconti performed several studies aimed at experimentally measuring the strain response of intact bones using SGs [8], [13], [35]. The strain distribution in the proximal human femoral metaphysis was measured in different configurations resembling single leg stance, using non-destructive tests [36]. A force corresponding to 0.75 BW was applied, and bone was assumed to behave linearly until 2.5 BW. Eleven triaxial stacked SGs (3x1.3 mm rectangular grid, 10x10 mm measuring grid carrier) were bonded to different locations (4 around the head, 3 around the neck, and 4 around the proximal diaphysis). The area for strain measurement was prepared by first degreasing it with ethanol, and then with a cocktail of acetone and 2-propanol. Then, the pores in the bone were filled, and the bone surface was waterproofed with two layers of polyurethane. Any excess of polyurethane was removed with fine sandpaper, and the SG bonded with cyanoacrylate glue. Finally, three layers of polyurethane were applied over each SG to protect their electrical circuits from water. Strains were sampled at 100 Hz (with a low-pass cut-off of 10 Hz). Major principal strains, minor principal strains, and the angle of the principal strains were computed. The SG reinforcement effect [37] was estimated with FE analyses, and was found to vary from region

to region, ranging from < 1% up to 15%. Such effect was more pronounced where the cortex was thinner (reinforcement lower than 4% for bone thicker than 1 mm).

A similar approach was recently proposed by the same group for a sideways fall configuration [35]. Sixteen SGs were bonded to one cadaver human femur, following the same protocol described above (one SG added on the lateral side of the femoral neck). Non-destructive tests were performed for twelve different sideways fall configurations, as well as in six different single leg stance configurations. Each of the non-destructive loading case was repeated six times. The specimens were eventually tested up to fracture in sideways fall. The study analysed the repeatability of the measurements, showing that differences between different loading configurations were two-three orders of magnitude larger than the variability between repetitions of the same loading configuration.

2.2 Fibre Bragg grating sensors

Fibre Bragg gratings were discovered in 1978, with the first fibre Bragg grating sensors (FBGS) commercialized in 1995. Applications to bone biomechanics were reported in the late 2000s, with the aim of measuring strains at the interface between two materials, e.g. bone and a prosthesis. Such measurements would not be possible with traditional SGs, whose electrical circuitry would be damaged, or with optical methods, since the materials under examination are not transparent [38].

2.2.1 Working principles. A FBGS consists of a fibre with different refraction indexes in the inner and the outer core. Stretching an FBGS changes its grating period, resulting in a change in wavelength of the reflected ultraviolet light. This change in wavelength is related to the change in the spatial period of the refractive index modulation using Bragg's law, which can be written in the form [39]: $\lambda_B = 2n_{eff}\Lambda$, where λ_B is the Bragg wavelength of the FBGS, η_{eff} is the effective refractive index of the fibre, and Λ is the periodicity of the grating. Thus, a longitudinal deformation can change both Λ and η_{eff}, the latter by the photo-elastic effect and the former by increasing the pitch of the grating. This causes a change in λ_B, which can be related to the applied longitudinal strain via: $\Delta\lambda_B / \lambda_B = (1-\rho_e)$. By knowing the photoelastic coefficient ρ_e, strains can be derived.

2.2.2 Most relevant studies. From the PubMed search, 26 publications were retrieved, where of 2 were considered relevant (Table 1). Fresvig et al. [38] addressed the suitability of FBGSs for strain measurement on bones by comparing them with SGs. Tests were conducted on an acryl tube and on human femur diaphysis. Both were reduced to a cylindrical shape, and 4 SGs and 4 FBGSs were mounted with a 45° relative shift. The specimens were compressed step-wise, and the longitudinal strains from SGs and FBGSs were recorded. No significant differences were found between the measured strains on the acrylic tube (Pearson correlation coefficients between sensors ranged from 0.986 - 1.0) or the cylindrical bone sample (Pearson correlation coefficient from 0.629 - 0.999). However, the standard deviation of the difference between FBGSs was not provided, as the different sensors were not subjected to the same deformation due to alignment inaccuracies of both the gauge and loading axis.

Reikeras et al. [40] continued from the conclusions of Fresvig [38], and used FBGSs to measure the strains at the implant-cortex interface of a cadaver femur with an implanted stem prosthesis. SGs were used to measure the strains on the external cortex. To prepare the bone for FBGS measurements, four shallow vertical ditches were made in the endosteal cortex (corresponding to the position and longitudinal direction of the rosette vertical SGs on the outside periosteal cortex). FBGSs were mounted in the ditches and bonded with cyanoacrylic adhesive. The stem of the prosthesis was not interfering with the FBGSs. The principal strains from the SGs were compared with

the single direction strain measurements of the corresponding FBGSs, under the assumption of the principal strain direction being aligned with the vertical axis.

2.3 Digital Image Correlation

The first formulations of digital image correlation (DIC) to measure deformations are from 1980s [41], [42]. DIC was initially adopted for measurements of large displacements/strains. The evolution of digital imaging devices with high resolution and increased frame rate recently allowed DIC to be used to detect strains on the order of a few hundred microstrains. Thus, applications of DIC in the field of bone mechanics are very recent.

2.3.1 Working principles. Digital image correlation is a non-contact method where one digital image is mapped onto another digital image. The images show the specimen that is tested, and the transformation field between the two images is used to retrieve the displacement field on the surface of the specimen. The transformation field is determined by maximizing a correlation coefficient. The latter is determined by examining pixel intensity array subsets on two or more corresponding images. The measurement accuracy of DIC can be affected by many factors, such as the size of the subset area used to match the same point in two images taken at different time points [43], the step size (i.e., the number of pixels by which the subset is shifted to calculate the strain field) and, if used, the type of data smoothing/filtering adopted.

DIC measurements can be 2D (one camera used), or surface-3D (two cameras used in stereovision). The full 3D approach (where a 3D imaging device, e.g. an X-ray tomograph, is used) is referred as Digital Volume Correlation (DVC), and is treated separately in this review.

2.3.2 Most relevant studies. From the PubMed search, 78 publications were retrieved, where of five were considered relevant (Table 1). Op Den Buijs and Dragomir-Daescu [44] used 2D DIC to measure displacements and strains over 22 cadaver femora. The bones were tested in a configuration resembling a fall to the side, at a displacement rate of 100 mm/s up to fracture. Images were recorded with a high-speed video camera (1024x512 px, 6000 fps). However, results of the measured strains were only qualitatively presented for two representative femora. Also, no description of the applied speckle pattern (if any) and image correlation algorithm used for analysis was provided.

Gilchrist et al. [45] assessed the capability of DIC to accurately measure strains on bones by comparing the strains measured by DIC to the measurements from SGs, considered as a gold standard. To do so, 20 human proximal femora were prepared with a strain rosette glued on the antero-superior femoral neck, and a speckle pattern was airbrushed over the same area. Femora were loaded to 50% of their predicted fracture load (determined using the method proposed by Boehm et al., [46]) at 0.5 mm/s. Images were recorded at 100 fps with 1280x800 px (approx. 17 px/mm) resolution. Minor principal strains were used for validation. Results showed a good correlation (Root mean square average difference 127 με, standard deviation 239 με), but also the presence of random image-to-image noise in the DIC data. The strains were only compared at one single location (anterior-superior aspect of the femoral neck), and at one time frame (corresponding to the maximal force in the test). Thereafter, DIC was used to measure strains in an impact simulator of sideways falls. However, DIC strain measurements recorded during the simulated fall on the side were not shown in the paper, and the authors only reported that strain fields calculated by DIC exhibited steep strain gradients, which were attributed to bone inhomogeneity.

Helgason et al. [47] performed a drop tower test over one proximal human femur specimen in a sideways fall configuration. The impact between the 16.5 kg impactor and the specimen occurred at a 3.5 m/s speed. Two high-speed cameras recorded the proximal femur anteriorly and posteriorly

(two separate 2D DIC set-up) at 9009 fps, 384x384 px (pixel pitch = 0.25 mm). However, the strains measured were only qualitatively compared to the predictions of FE models (minimum principal strains on the anterior surface shown), and no quantitative data was reported from the strain measurements.

Grassi et al. [48] recently performed a study investigating the strain response of three human cadaver femora at physiological-like strain rates. Two high-speed (3000 fps) cameras were used in a surface 3D DIC scheme, and different correlation settings were used to analyse the whole load curve and the near-fracture behaviour. Those correlation settings were determined from an undeformed control plate which was used as a noise level reference during the tests. A data filtering method was developed, in which the obtained displacement vectors for each point were filtered in time using a low-pass filter. The filtered displacements were then used to calculate the strains. Digital SGs were identified and their output compared with literature. The evolution of the principal strain magnitude and direction was analysed at different stages of the loading curve, and the collected data can act as a quantitative and comprehensive benchmark for numerical models.

Tang et al. [49] investigated the mechanical behaviour of human cortical bone at the tissue level under shear. They used, among other techniques, 2D DIC to map the surface strains during the shear test. Polished 20x5x3 mm bone samples with two V-shaped notches were obtained and tested under pure shear up to fracture at a 0.2 mm/min displacement rate. Strains were measured on a 3.6x2.7 mm section using an optical microscope equipped with a digital camera (4 fps). Use of optical microscope images together with the intrinsic microstructural features of the polished samples provided a contrasted enough pattern in the acquired digital images, so no artificial speckle pattern was needed.

2.4 Digital Volume Correlation

Digital volume correlation (DVC) for tomographic datasets was first proposed by Bay et al. in 1999 [50]. They proposed that the 2D-DIC concepts could be extended to match small sub-volumes of a tomographic reconstruction before and after undergoing loading to obtain a full volumetric field of 3D motions. DVC applications in bone mechanics are thus very recent.

2.4.1 Working principles. DVC is essentially the 3D extension of the 2D-DIC method. In 2D-DIC, a coefficient based on the summed difference of intensity values in a subset of a planar images is minimized. In DVC, the minimization is done on a 3D-subset where intensity values corresponding to (x,y,z) values are compared to a standard and the summed difference minimized using the predictive 3D displacement fields. Since tomographic attenuation-based images are used, a “white light” speckle pattern is not available, and DVC relies on naturally occurring patterns of the specimen to track changes in material features.

2.4.2 Most relevant studies. Thirteen publications were retrieved, where of five were relevant (Table 1). Since only a limited number of publications on DVC in bone mechanics was available, some experimental studies performed on non-human bones were also included.

Roberts et al. [23] recently reviewed the application of DVC on trabecular bone, with the aim of clarifying the role of the different correlation parameters on the outcome. The main conclusions were:

- Subset size is the most influential parameter in terms of measurement precision

- A global correlation approach can reduce displacement measurement error compared to local techniques. This is accomplished by imposing continuity requirements, such that mapping of a single subset depends on mapping of adjacent regions.
- Since it is not possible to apply an artificial speckle pattern inside a specimen, the accuracy and precision of displacement and strain measurement are affected by the different bone micro-structure (e.g., bone volume fraction, trabecular number and separation, structure model index).

Hussein et al. [51] used DVC to investigate the mechanics of 30 L1 vertebrae. To the authors' knowledge, this is the first and solely study reporting the usage of DVC on human bones at the organ level. The L1 segments were first preconditioned ten times at 400 N, and were then imaged with a µCT. Step-wise 1 mm displacements were applied allowing 20 min relaxation time between steps. Samples were µCT scanned after each step (µCT80, Scanco Medical, 37 µm voxel size, 70 kVp, 114 mA, and 300 ms integration time). A final µCT scan was performed after fracture. A hexahedral mesh was created from the segmented vertebral geometries. The elements of the mesh defined the subsets used for DVC calculations. The correlation between subsets was calculated using a maximum likelihood method. Accuracy and precision were high when using simulated displacements (mean-bias error and root-mean-square error for the displacement about 0.025% and 0.35%, respectively). However, errors increased when real image data from repeated µCT acquisitions were used. This might have been due to imaging inaccuracies, such as X-ray beam fluctuations, or repositioning errors, which together led to a discrepancy between repeated measurements of 740 ± 630 µε (0.58 ± 1.12 voxels displacement).

The need for accurate quantification of the measurement inaccuracies in DVC measurements was addressed by Gillard et al. [16], with a study on porcine trabecular bone. Five repeated µCT scans were performed (HMX ST, Nikon Metrology, 24.6 µm voxel size, 105 kVp) on the same specimen, the first three without moving the sample, and the last two after shifting it by 125 µm in the vertical direction. DVC was calculated using a local approach (i.e., the shift of the pattern within each subset is independent from the shift of the neighbouring subsets) based on the fast Fourier transform (FFT). Strain resolutions ranging between 70 µε and 800 µε were reported when using the identified optimal correlation parameters (64 voxels sub-volume size, 50% overlap). More in detail, repeated scans without repositioning led to an accuracy (average strain) and precision (standard deviation of the strain) of 40 and 140 µε, respectively. When the specimens were repositioned between scans, the reported accuracy and precision were 250 and 750 µε, respectively. A significant decrease in the sub-volumes correlation was also reported when the trabeculae started to yield or fail. This led to unrealistic strain values, and the authors proposed to cut out points whose correlation values are below 0.9.

Dall'Ara et al. [52] performed a methodological study aimed at evaluating precision and accuracy of DVC strain measurement on bovine cortical and trabecular bone specimens (3 mm in diameter, 29 mm in length) imaged with µCT (Skyscan 1172, Bruker, 10 µm voxel size, 59-70 kV, 1180 ms exposure time). A custom global (i.e., the displacement of each subset is affected by the displacements of its neighbouring elements) DVC algorithm was used based on the ShIRT library [53] for deformable image registration. Briefly, an elastic registration algorithm was coupled to a FE simulation to calculate the strains in the mesh. Accuracy and precision were analysed by comparing virtually displaced scans, repeated scans without any repositioning of the sample, and repeated scans taken after sample repositioning. The authors concluded that the main source of error was the intrinsic noise of the µCT images. The error in the measurement could be decreased by increasing the size of the grid for strain calculation (a power law relationship between the two is reported), paying the

price of decreased spatial resolution. For a grid size of 50 px, the accuracy and precision ranges reported were 425-692 με and 202-394 με, respectively. Performing DVC on cortical bone resulted in a 10-25% decrease in the accuracy compared to trabecular bone with identical procedure. Therefore, the authors suggested that DVC strain measurements could be used to efficiently discriminate yielded from non-yielded regions. Reaching the accuracy needed to investigate the elastic regime required an increase of the grid size that would have ultimately reduced the spatial resolution too much.

Palanca et al. [54] compared the performances of three different DVC algorithms on two cylindrical samples of cortical and trabecular bone, respectively. The samples were imaged with μCT (Skyscan 1172, Bruker, 10 μm voxel size, 59-70 kV, 1180 ms exposure time). Most likely, the same datasets as in Dall'Ara et al. [52] were used in this study. The three algorithms evaluated in this study were: two proprietary codes (LaVision Ltd, Germany) based on FFT and direct correlation (DC), respectively, and the ShIRT-based approach proposed in [52]. The comparison was performed in terms of strain accuracy (average strain) and precision (standard deviation), both against repeated scans without repositioning, and virtually displaced volumes. The FFT-based DVC exhibited a much faster computation time, but also the worst accuracy (one order of magnitude difference with respect to the other two methods) and precision. Both ShIRT- and DC-based DVC algorithm had accuracy and precision in the order of a few hundred microstrains when the optimal parameters (50 voxels subset size) were adopted. In general, ShIRT-based DVC performed better than the other two algorithms, and the authors ascribed this to the global nature (which implies a continuity assumption) of the approach.

3. Discussion

The increasing number of studies aiming to model bone behaviour and bone fracture requires adequate validation methods. However, extracting relevant and accurate strain measurements from biomechanical experiments on bone is a challenge. The aim of the present review was to examine the most relevant literature regarding strain measurements on human bone samples ex vivo, with focus on the organ- and tissue-level. Each relevant technique was presented with an emphasis on the additional complexity introduced by having bone as the substrate material.

The comparison between experimental studies and different strain measurement techniques was somewhat impaired by the lack of a commonly defined metrics. In an attempt to compare the methods, we chose to report sampling frequency, spatial resolution, and strain accuracy for the studies where such data was available (Table 2). Please observe that the values for strain accuracy might have been defined in different ways for different techniques, and sometimes between different studies adopting the same technique. Therefore, references were provided for each reported value, and the reader is encouraged to check the referred papers to get a more detailed definition.

3.1 Strain gauges

SGs are often considered the gold standard for strain measurements on bone. However, obtaining accurate strain data with SGs is not trivial. Bone characteristics do not naturally meet the requirements for optimal SG adhesion [29], and the procedures to optimize bone surface for SG measurements require training and skills. Moreover, SG measurement on bone presents intrinsic limitations. The first is the discreteness of the measurement. SGs can only record the average strain of the area to which they are bonded. The number of SGs that can be applied over a sample is limited by practical obstacles, e.g., limited presence of flat enough areas over the bone surface, electrical wires hindrance, etc. This results in having typically no more than 20 SGs applied over a proximal

femur sample. Besides, the SG location has to be determined beforehand. Such position is usually determined either through numerical simulations, or by pursuing consistency with previous literature. This is an important limitation when the strains leading to, e.g., yielding or crack formation are investigated. Finally, SGs themselves have non-negligible stiffness, which leads to the so-called "reinforcement effect" [37]. The entity of the reinforcement can be calculated theoretically under certain conditions [55], [56], and has been estimated to be up to 15% on thin cortical sections of a femur using a validated FE procedure [36].

3.2 Fibre Bragg grating sensors

The main advantages of FBGSs are small size, light weight, biocompatibility, chemical inertness, and immunity to electromagnetic interference. Most of these qualities represent a significant advantage for *in vivo* application of FBGSs. As for the *ex vivo* applications, the main advantage of FBGSs is the absence of damageable electrical circuitry, that allows their positioning for example at the interface between two materials. This makes FBGSs a valuable option to investigate the strain response at the bone/implant interface. The potential of such application was shown by Reikeras et al. [40], who found that deformations on the external cortex and the internal cortex at the bone/implant interface are not related. Thus, it is important to measure strains directly at the bone/implant interface to eventually improve implant design. Despite FBGSs are commercially available in a rosette configuration (thus being able to measure principal components of strain, analogously to SGs), the only two applications found in bone mechanics used single-fibre FBGSs. This represents a limitation to those studies, as the hypothesis of principal strains being aligned to the shaft axis is likely not to hold at the bone-implant interface.

A few studies have compared the accuracy of FBGSs and SGs, where SGs provided a higher precision [39]. Fresvig et al. [38] reported non-significant differences between SG and FBGS, but a direct quantitative comparison was not provided. While SGs attain a high linearity in the response, FBGSs have a different sensitivity between positive and negative loads, and a very high sensitivity to temperature gradients [17]. Di Sante et al. [57] reported that the sensitivity values for FBGSs may differ significantly from the theoretical value for silica fibers, and recommended an in-situ calibration against a gold standard. Further development of the sensor technology, together with a more refined set-up for the application to bone material can possibly lead to an accuracy approaching that of SGs.

3.3 Digital image correlation

DIC has some advantages over the methods discussed above. First is the potential to obtain the full-field strain response of the bone, rather than a finite number of discrete strain measurements. A second advantage is the non-contact nature of DIC, which reduces the reinforcement effect to a minimum (or even completely eliminates it if no paint is applied [49]). Last, the rapid development of digital imaging technology results in the possibility of obtaining more accurate spatial and time resolved strain data. Despite these advantages, DIC has been scarcely used in ex vivo experiments, and no consensus exists on its reliability for bone mechanics. This is mostly due to the lack of methodological studies conducted with DIC on bone samples. Such studies are limited to 2D-DIC studies evaluated using synthetic images [18], [58], [59], thus not considering the spectrum of additional complexities introduced by testing human bone samples (e.g., non-planar, rough and wet surfaces, tracked using a 3D-surface DIC approach). Only Gilchrist et al. [45] performed a validation of DIC on bone against one SG.

Most experimental studies using DIC adopted a 2D approach over femoral bone specimens [44], [47]. This approach likely introduces significant artefacts in the measured strains as soon as the normal to the bone surface deviates from the optical axis of the camera. This limited the authors to a

qualitative analysis of the measured DIC data. Such 2D DIC approach is instead suitable for studies involving regular shape, polished bone samples as in Tang et al. [49]. Another potential issue with DIC is linked to its continuum nature. DIC in its original formulation [43] inherently assumes that the object under consideration shows no strong discontinuities in displacement between consecutive images. This condition is clearly violated when a crack is formed on the specimen, and suggests additional care when dealing with DIC measurements from dynamic impact tests, such as in, e.g., [45], [47]. Thus, care must be taken to exclude regions where the continuum hypothesis is violated, unless extended DIC formulations are adopted [60], [61]. However, such extended DIC formulations are still under development, and out of the scope of the present review.

A proper application of DIC requires that the correlation parameters are optimized for that specific application. That implies that an a priori optimal set of parameters does not exist, nor does a univocal formula to calculate them. Some general guidelines about the choice of the correlation parameters (subset size, step size, and filtering) can be found in, e.g., Sutton et al.,[43]. In simple terms, the larger a subset is, the more information it will contain, thus increasing the likelihood of obtaining a good correlation. On the other hand, an increase of the subset size leads to a decreased spatial resolution. Analogously, an increase of the step size will reduce the noise in the calculated strains, but will reduce the spatial resolution. Ultimately this results in the need to find an optimal trade-off between the parameters, which may require both experience and a considerable amount of trials.

One last concern with DIC is the determination of spatial resolution of the extracted displacement/strain field. The spatial resolution of DIC data is driven by the spatial resolution of the acquired images (in terms of px/mm ratio). However, the final resolution of the strain measurements depends on a number of other factors, like optical lens quality, marker size [62], and the correlation algorithm/parameters adopted. The absence of a univocal definition for the spatial resolution leads to that DIC spatial resolution is not reported, potentially impairing the clarity of the reported results, and the possibility to compare different studies.

3.4 Digital volume correlation

Digital volume correlation is the extension of 2D-DIC to the third spatial dimension. Thus, the same considerations as for DIC still holds. Although DVC can be performed on different type of 3D images (e.g. magnetic resonance, confocal microscopy, optical coherence tomography), applications to bone biomechanics at the organ and tissue level have only been reported using CT images. When compared to DIC with digital images, the use of X-ray tomographic reconstructions to calculate the strain field leads to two additional sources of noise, namely: (i) the noise of the tomographic images, which is generally higher than that of digital images, and (ii) that it is impossible to apply an artificial speckle pattern to enhance the correlation. The majority of studies adopting DVC on bone samples [16], [23], [51], investigated bone mechanical properties at the tissue-level. This is because the trabecular bone at the tissue-level consists of a spongy network which is very well suitable for the calculation of a correlation coefficient between subsets of such network. The reported ranges of accuracy and precision for DVC strain measurements on trabecular bone samples are 20-1,280 με and 39-630 με, respectively (extrapolated from [52]). Only one DVC study investigated human bone at the organ level by scanning whole L1 vertebra samples [51]. However, the level of noise between repeated acquisitions of an undeformed sample was greater than 740±630 με. This value is only ten times lower than the yield strain reported for trabecular bone in vertebrae [63], thus impairing the investigation of strains at physiological load levels. Dall'Ara et al. [52] evidenced that both the precision and accuracy errors decrease with a power law as a function of the increasing size of the correlation window. However, increasing the size of the correlation window leads to a loss of spatial resolution. This poses the problem of finding the best compromise between spatial resolution and

strain resolution for the designed study. The noise of the DVC measurements was also found to be related to the intrinsic noise of the tomographic images. Dall'Ara et al. [52] also compared their accuracy and precision with those achieved by [16] when equivalent correlation parameters (two different DVC approaches were adopted in the two studies) were used. They found that the FFT-DVC approach in [16] achieved a better accuracy in the stationary test (i.e., repeated scans without repositioning), whereas the method by [52] performed better in when the specimen was repositioned after the first scan.

The relevant issue of comparing the performances of different DVC algorithms on a common set of data was only recently addressed by Palanca et al. [54]. The study showed that a DVC approach implementing a continuity constraint between neighbouring subsets provided a higher strain accuracy and precision than local DVC approaches when evaluated using repeated scans without repositioning, in agreement with [23]. Another important aspect that should be addressed is the optimal image resolution for DVC, i.e., what image resolution is good enough to achieve a high correlation between the subsets while not having an unnecessarily high X-ray dose or long scanning time. To our best knowledge, no study has addressed this question for bone samples yet.

The results reported in the evaluated DVC studies show that accuracy and precision are both around 200 με when a subset size corresponding to ~700 μm is used [52]. Thus, the strains during the elastic regime cannot be measured with a proper accuracy with current methodology. It is instead possible to successfully use DVC to discern yielded areas, and to measure strains around the yield point. However, it has to be observed that measuring over the yield point has other drawbacks. It is in fact not possible to obtain a good correlation value between excessively distorted subsets [16].

In summary, DVC is a very powerful tool to explore the full field 3D strain distribution in bone samples. However, two main issues have to be solved: (i) the noise levels in μCT scans, and (ii) the time needed to acquire one μCT volume. As for the first issue, use of synchrotron-based tomographic scanners can possibly contribute to address such limitation in the immediate future. Although providing a limited field-of-view, synchrotron-based tomographic scanners allow for higher image resolutions and less noisy image due to the higher brilliance and collimation of the X-ray source. As for the time needed to acquire one CT volume, this currently represents a severe limitation to DVC studies, as a full scan can take up to several hours. This means that the real time bone response, as well as creep and stress relaxation effects in bone cannot be investigated.

4. Conclusions

The scope of this review was to provide the means to decide which of the reviewed methods best fits the needs of the reader's experiment. It appears evident that no method is clearly superior to the others. However, the following conclusions can be drawn:

- Despite being old, SGs are still the gold standard when it comes to strain accuracy and measurement repeatability. They are recommended for accurate, discrete measurements in specific locations that can be a priori determined.
- FBGSs have lower precision and accuracy than SGs. FBGSs are recommended for regions where SG application is impaired by practical reasons. The interface between internal bone cortex and an artificial implant is a typical example of this.
- DIC presents advantages over SGs, including but not limited to the higher number of measurements, which allows for the reconstruction of full-field strain patterns. However, the estimation of the spatial resolution of DIC measurements is not trivial, and noise has to be handled with care. Therefore, future studies adopting DIC should report all the details of

their procedure, especially including the parameters chosen to calculate the correlation coefficients (subset size, step size, etc.)

- Digital volume correlation can augment the knowledge in terms of internal strain distribution in bone in response to different loading conditions and when approaching yield. However, DVC is sensitive to noise in the obtained strain data. Such noise effects need to be controlled and measured in order to get a proper strain resolution. Moreover, the long acquisition time currently limits the usability to experiments where the real time strain response is not crucial.

References

[1] D. D. Cody, G. J. Gross, F. J. Hou, H. J. Spencer, S. A. Goldstein, and D. P. Fyhrie, "Femoral strength is better predicted by finite element models than QCT and DXA," *J Biomech*, vol. 32, no. 10, pp. 1013–1020, 1999.

[2] R. Huiskes and E. Y. S. Chao, "A survey of finite element analysis in orthopedic biomechanics: The first decade," *J. Biomech.*, vol. 16, no. 6, pp. 385–409, Jan. 1983.

[3] P. Prendergast, "Finite element models in tissue mechanics and orthopaedic implant design," *Clin. Biomech.*, vol. 12, no. 6, pp. 343–366, Sep. 1997.

[4] A. N. Natali and E. A. Meroi, "A review of the biomechanical properties of bone as a material," *J. Biomed. Eng.*, vol. 11, no. 4, pp. 266–276, Jul. 1989.

[5] L. Peng, J. Bai, X. Zeng, and Y. Zhou, "Comparison of isotropic and orthotropic material property assignments on femoral finite element models under two loading conditions.," *Med. Eng. Phys.*, vol. 28, no. 3, pp. 227–33, Apr. 2006.

[6] P. Zysset, "A review of morphology–elasticity relationships in human trabecular bone: theories and experiments," *J. Biomech.*, vol. 36, no. 10, pp. 1469–1485, 2003.

[7] B. Helgason, E. Perilli, E. Schileo, F. Taddei, S. Brynjólfsson, and M. Viceconti, "Mathematical relationships between bone density and mechanical properties: a literature review.," *Clin. Biomech. (Bristol, Avon)*, vol. 23, no. 2, pp. 135–46, Feb. 2008.

[8] L. Cristofolini, F. Taddei, M. Baleani, F. Baruffaldi, S. Stea, and M. Viceconti, "Multiscale investigation of the functional properties of the human femur.," *Philos. Trans. A. Math. Phys. Eng. Sci.*, vol. 366, no. 1879, pp. 3319–41, Sep. 2008.

[9] M. Ding and M. Dalstra, "Age variations in the properties of human tibial trabecular bone," *J. Bone …*, pp. 995–1002, 1997.

[10] D. Webster and R. Müller, “In silico models of bone remodeling from macro to nano--from organ to cell.,” *Wiley Interdiscip. Rev. Syst. Biol. Med.*, vol. 3, no. 2, pp. 241–51, Jan. .

[11] A. G. Robling, A. B. Castillo, and C. H. Turner, “Biomechanical and molecular regulation of bone remodeling.,” *Annu. Rev. Biomed. Eng.*, vol. 8, pp. 455–98, Jan. 2006.

[12] M. Viceconti, S. Olsen, L.-P. Nolte, and K. Burton, “Extracting clinically relevant data from finite element simulations.,” *Clin. Biomech. (Bristol, Avon)*, vol. 20, no. 5, pp. 451–4, Jun. 2005.

[13] L. Cristofolini, E. Schileo, M. Juszczyk, F. Taddei, S. Martelli, and M. Viceconti, “Mechanical testing of bones: the positive synergy of finite-element models and in vitro experiments.,” *Philos. Trans. A. Math. Phys. Eng. Sci.*, vol. 368, no. 1920, pp. 2725–63, Jun. 2010.

[14] A. E. Anderson, B. J. Ellis, and J. A. Weiss, “Verification, validation and sensitivity studies in computational biomechanics.,” *Comput. Methods Biomech. Biomed. Engin.*, vol. 10, no. 3, pp. 171–84, Jun. 2007.

[15] N. P. Klokova, “Metrological characteristics of resistance strain gauges and evaluation of deformation measurement errors,” *Meas. Tech.*, vol. 21, no. 5, pp. 640–649, May 1978.

[16] F. Gillard, R. Boardman, M. Mavrogordato, D. Hollis, I. Sinclair, F. Pierron, and M. Browne, “The application of digital volume correlation (DVC) to study the microstructural behaviour of trabecular bone during compression.,” *J. Mech. Behav. Biomed. Mater.*, vol. 29, pp. 480–99, Jan. 2014.

[17] T. Kleckers, “Fibre Bragg sensors compared with electrical strain gauges for use in force measurement - Prospects and potentials,” in *XIX IMEKO World Congress Fundamental and Applied Metrology*, 2009.

[18] M. Bornert, F. Brémand, P. Doumalin, J.-C. Dupré, M. Fazzini, M. Grédiac, F. Hild, S. Mistou, J. Molimard, J.-J. Orteu, L. Robert, Y. Surrel, P. Vacher, and B. Wattrisse, “Assessment of Digital Image Correlation Measurement Errors: Methodology and Results,” *Exp. Mech.*, vol. 49, no. 3, pp. 353–370, Dec. 2009.

[19] D. J. Pratt, P. Bowker, D. Wardlaw, and J. McLauchlan, “Load measurement in orthopaedics using strain gauges,” *J. Biomed. Eng.*, vol. 1, no. 4, pp. 287–296, Oct. 1979.

[20] R. Bedzinski and M. Tyndyk, “Experimental methods of stress and strain analysis in orthopaedics biomechanics,” *Acta Bioeng. Biomech.*, vol. 2, no. 2, 2000.

[21] E. Gdoutos, D. Raftopoulos, and J. Baril, “A critical review of the biomechanical stress analysis of the human femur,” *Biomaterials*, vol. 3, pp. 2–8, 1982.

[22] B. Ovryn, “Whole-field displacement and strain measurements: application to biomechanics,” *OE/LASE’93 Opt. Electro-Optics, …*, vol. 1889, 1993.

[23] B. C. Roberts, E. Perilli, and K. J. Reynolds, “A Review on the Application of the Digital Volume Correlation Technique for the Measurement of Displacement and Strain Fields in Bone,” *J. Biomech.*, vol. 47, no. 5, Jan. 2014.

[24] A. Miles and K. Tanner, *Strain measurement in biomechanics*. Dordrecht: Springer Netherlands, 1992.

[25] Y. An and R. Draughn, *Mechanical testing of bone and the bone-implant interface*. 1999.

[26] T. Meling, K. Harboe, and K. Søreide, "Incidence of traumatic long-bone fractures requiring in-hospital management: a prospective age- and gender-specific analysis of 4890 fractures.," *Injury*, vol. 40, no. 11, pp. 1212–1219, 2009.

[27] E. S. Gurdjian and H. R. Lissner, "Mechanism of Head Injury as Studies by the Cathode Ray Oscilloscope Preliminary Report," *J. Neurosurg.*, vol. 1, no. 6, pp. 393–399, 1944.

[28] I. Kyowa Electronic Instruments, "Strain gage catalogue." pp. 1–100.

[29] V. Micro-Measurements, "Surface preparation for strain gage bonding," *Online Doc.*, no. 11129, pp. 1–7, 2009.

[30] V. L. Roberts, "Strain-gage techniques in biomechanics," *Exp. Mech.*, vol. 6, no. 3, p. 19A–22A, Mar. 1966.

[31] Y. H. Kim, J. S. Kim, and S. H. Cho, "Strain distribution in the proximal human femur. An in vitro comparison in the intact femur and after insertion of reference and experimental femoral stems.," *J. Bone Joint Surg. Br.*, vol. 83, no. 2, pp. 295–301, Mar. 2001.

[32] A. Aamodt, J. Lund-Larsen, J. Eine, E. Andersen, P. Benum, and O. S. Husby, "Changes in proximal femoral strain after insertion of uncemented standard and customised femoral stems," *J. Bone Jt. Surg.*, vol. 83, no. 6, pp. 921–929, Aug. 2001.

[33] T. Basso, J. Klaksvik, U. Syversen, and O. A. Foss, "A biomechanical comparison of composite femurs and cadaver femurs used in experiments on operated hip fractures.," *J. Biomech.*, vol. 47, no. 16, pp. 3898–902, Dec. 2014.

[34] P. O. Østbyhaug, J. Klaksvik, P. Romundstad, and A. Aamodt, "An in vitro study of the strain distribution in human femora with anatomical and customised femoral stems.," *J. Bone Joint Surg. Br.*, vol. 91, no. 5, pp. 676–82, May 2009.

[35] L. Zani, P. Erani, L. Grassi, F. Taddei, and L. Cristofolini, "Strain distribution in the proximal Human femur during in vitro simulated sideways fall," *J. Biomech.*, 2015.

[36] L. Cristofolini, M. Juszczyk, F. Taddei, and M. Viceconti, "Strain distribution in the proximal human femoral metaphysis.," *Proc. Inst. Mech. Eng. H.*, vol. 223, no. 3, pp. 273–88, Apr. 2009.

[37] C. C. Perry, "Strain-gage reinforcement effects on orthotropic materials," *Exp. Tech.*, vol. 10, no. 2, pp. 20–24, 1986.

[38] T. Fresvig, P. Ludvigsen, H. Steen, and O. Reikerås, "Fibre optic Bragg grating sensors: an alternative method to strain gauges for measuring deformation in bone.," *Med. Eng. Phys.*, vol. 30, no. 1, pp. 104–8, Jan. 2008.

[39] M. Werneck, R. Allil, B. Ribeiro, and F. de Nazaré, "A Guide to Fiber Bragg Grating Sensors," pp. 1–24, 2013.

[40] O. Reikeras, G. T. Aarnes, H. Steen, P. Ludvigsen, and G. Sagvolden, “Differences in external and internal cortical strain with prosthesis in the femur.,” *Open Orthop. J.*, vol. 5, pp. 379–84, Jan. 2011.

[41] M. Sutton, W. Wolters, W. Peters, W. Ranson, and S. McNeill, “Determination of displacements using an improved digital correlation method,” *Image Vis. Comput.*, vol. 1, no. 3, pp. 133–139, Aug. 1983.

[42] W. Peters and W. Ranson, “Digital imaging techniques in experimental stress analysis,” *Opt. Eng.*, vol. 21, no. 3, p. 213427, Jun. 1982.

[43] M. A. Sutton, J. J. Orteu, and H. Schreier, *Image Correlation for Shape, Motion and Deformation Measurements: Basic Concepts, Theory and Applications*. Springer, 2009.

[44] J. Op Den Buijs and D. Dragomir-Daescu, “Validated finite element models of the proximal femur using two-dimensional projected geometry and bone density.,” *Comput. Methods Programs Biomed.*, vol. 104, no. 2, pp. 168–74, Nov. 2011.

[45] S. Gilchrist, P. Guy, and P. a Cripton, “Development of an inertia-driven model of sideways fall for detailed study of femur fracture mechanics.,” *J. Biomech. Eng.*, vol. 135, no. 12, p. 121001, Dec. 2013.

[46] H. F. Boehm, A. Horng, M. Notohamiprodjo, F. Eckstein, D. Burklein, A. Panteleon, J. Lutz, and M. Reiser, “Prediction of the fracture load of whole proximal femur specimens by topological analysis of the mineral distribution in DXA-scan images,” *Bone*, vol. 43, no. 5, pp. 826–831, 2008.

[47] B. Helgason, S Gilchrist, O. Ariza, J. D. Chak, G. Zheng, R. P. Widmer, S. J. Ferguson, P. Guy, and P. a Cripton, “Development of a balanced experimental-computational approach to understanding the mechanics of proximal femur fractures.,” *Med. Eng. Phys.*, vol. 36, no. 6, pp. 793–799, Mar. 2014.

[48] L. Grassi, S. P. Väänänen, S. Amin Yavari, J. S. Jurvelin, H. Weinans, M. Ristinmaa, A. A. Zadpoor, and H. Isaksson, “Full-field Strain Measurement During Mechanical Testing of the Human Femur at Physiologically Relevant Strain Rates,” *J. Biomech. Eng.*, vol. 136, no. 11, 2014.

[49] T. Tang, V. Ebacher, P. Cripton, P. Guy, H. McKay, and R. Wang, “Shear deformation and fracture of human cortical bone.,” *Bone*, vol. 71, pp. 25–35, Feb. 2015.

[50] B. K. Bay, T. S. Smith, D. P. Fyhrie, and M. Saad, “Digital volume correlation: Three-dimensional strain mapping using X-ray tomography,” *Exp. Mech.*, vol. 39, no. 3, pp. 217–226, Sep. 1999.

[51] A. Hussein, P. Barbone, and E. Morgan, “Digital volume correlation for study of the mechanics of whole bones,” *Procedia IUTAM*, vol. 4, pp. 116–125, 2012.

[52] E. Dall’Ara, D. Barber, and M. Viceconti, “About the inevitable compromise between spatial resolution and accuracy of strain measurement for bone tissue: A 3D zero-strain study,” *J. Biomech.*, vol. 47, no. 12, Jul. 2014.

[53] D. C. Barber and D. R. Hose, “Automatic segmentation of medical images using image registration: diagnostic and simulation applications.,” *J. Med. Eng. Technol.*, vol. 29, no. 2, pp. 53–63, 2005.

[54] M. Palanca, G. Tozzi, L. Cristofolini, M. Viceconti, and E. Dall’Ara, “3D Local Measurements of Bone Strain and Displacement: Comparison of Three Digital Volume Correlation Approaches.,” *J. Biomech. Eng.*, Mar. 2015.

[55] M. F. Beatty and S. W. Chewning, “Numerical analysis of the reinforcement effect of a strain gage applied to a soft material,” *Int. J. Eng. Sci.*, vol. 17, no. 7, pp. 907–915, 1979.

[56] A. Ajovalasit, S. Fragapane, and B. Zuccarello, “Local reinforcement effect of embedded strain gauges,” *EPJ Web Conf.*, vol. 6, 2010.

[57] R. Di Sante, L. Donati, E. Troiani, and P. Proli, “Reliability and accuracy of embedded fiber Bragg grating sensors for strain monitoring in advanced composite structures,” *Met. Mater. Int.*, vol. 20, no. 3, pp. 537–543, May 2014.

[58] F. Amiot, M. Bornert, P. Doumalin, J.-C. Dupré, M. Fazzini, J.-J. Orteu, C. Poilâne, L. Robert, R. Rotinat, E. Toussaint, B. Wattrisse, and J. S. Wienin, “Assessment of Digital Image Correlation Measurement Accuracy in the Ultimate Error Regime: Main Results of a Collaborative Benchmark,” *Strain*, vol. 49, no. 6, pp. 483–496, Dec. 2013.

[59] B. Pan, K. Qian, and H. X. and Anand, “Two-dimensional digital image correlation for in-plane displacement and strain measurement: a review,” *Meas. Sci. Technol.*, vol. 20, no. 6, p. 62001, 2009.

[60] T. L. Nguyen, S. A. Hall, P. Vacher, and G. Viggiani, “Fracture mechanisms in soft rock: Identification and quantification of evolving displacement discontinuities by extended digital image correlation,” *Tectonophysics*, vol. 503, no. 1–2, pp. 117–128, Apr. 2011.

[61] S. Roux, J. Réthoré, and F. Hild, “Digital image correlation and fracture: an advanced technique for estimating stress intensity factors of 2D and 3D cracks,” *J. Phys. D. Appl. Phys.*, vol. 42, no. 21, p. 214004, Nov. 2009.

[62] G. Lionello and L. Cristofolini, “A practical approach to optimizing the preparation of speckle patterns for digital-image correlation,” *Meas. Sci. Technol.*, vol. 25, no. 10, p. 107001, Oct. 2014.

[63] D. Kopperdahl and T. M. Keaveny, “Yield strain behavior of trabecular bone,” *J. Biomech.*, vol. 31, no. 7, pp. 601–608, Jul. 1998.

[64] J. Op Den Buijs and D. Dragomir-Daescu, “Validated finite element models of the proximal femur using two-dimensional projected geometry and bone density.,” *Comput. Methods Programs Biomed.*, pp. 1–7, 2010.

[65] L. Grassi, S. P. Väänänen, S. Amin Yavari, H. Weinans, J. S. Jurvelin, A. a. Zadpoor, and H. Isaksson, “Experimental Validation Of Finite Element Model For Proximal Composite Femur Using Optical Measurements,” *J. Mech. Behav. Biomed. Mater.*, vol. 21, pp. 86–94, Feb. 2013.

[66] M. A. Sutton, “Three-dimensional digital image correlation to quantify deformation and crack-opening displacement in ductile aluminum under mixed-mode I/III loading,” *Opt. Eng.*, vol. 46, no. 5, p. 051003, May 2007.

[67] B. Pan, D. Wu, and L. Yu, “Optimization of a three-dimensional digital image correlation system for deformation measurements in extreme environments,” *Appl. Opt.*, vol. 51, no. 19, p. 4409, Jun. 2012.

TABLES

Table 1: Search criteria to retrieve the reviewed studies on PubMed. For each method, the search keywords used and the number of retrieved publications are reported, together with the detail of the eligible studies. Two publications non-indexed in PubMed were added in the strain gauges section.

	Keywords	**Retrieved publications**	**Eligible**	**References**
Strain gauges (SG)	(gauge OR gage OR distribution) AND human AND (femur OR femurs OR femora) AND strain	239	4+1	[31], [34]–[36] Extra: [30]
Fibre Bragg grating sensors (FBGS)	(bragg OR grating OR (optical AND (fibre OR fibre))) AND (bone OR femur OR femora) AND strain	26	2	[38], [40]
Digital image correlation (DIC)	(digital AND image AND correlation) AND (femur OR bone) AND (strain OR mechanics)	78	5	[45], [47]–[49], [64]
Digital Volume Correlation (DVC)	(digital AND volume AND correlation) AND (femur OR bone) AND (strain OR mechanics)	13	5	[16], [23], [51], [52], [54]

Table 2: Comparison of the performances of the four reviewed methods based on the reviewed studies. The spatial resolution was determined as the size of the excitation grids for the SG, and as the pixel/voxel size for DIC/DVC. Strain accuracy was reported when available (only indicative values).

	Sampling frequency [Hz]	**Spatial resolution***	**Type of measurement**	**Strain accuracy [με]**
Strain gauges	100 Hz [36]	3x1.25 mm grid size [31], [34] 3x1.3 mm grid size [36]	Contact, discrete	N/A
Optical Bragg grating fibre	60 Hz [40]	N/A	Contact, discrete	N/A
Digital image correlation	3000 Hz [65] - 9216 Hz [45] (100 Hz for DIC validation against SG [45])	5 px/mm [45], [47] - 10 px/mm [48] (17px/mm for DIC validation against SG [45])	Non-contact, full-field	~33 μ in the standing control plate [48]
Digital volume correlation	~ 3×10^{-4} (estimated by the authors)	12-82 μm voxel size [23]	Non-contact, full-field	740 μ [51] 20-250 μ [16] 10-792 μ [52]

FIGURES

Figure 1: The four strain measurement techniques reviewed: a) strain gauges, b) fibre Bragg grating sensors, c) digital image correlation, and d) digital volume correlation. For each of these techniques, a schematic of the working principle is shown on the right, and an example of application to bone mechanics is reported on the left side.

Parts of the figure are reprinted from [38], [66], [67] with permission of Elsevier, Spie, and IOP.

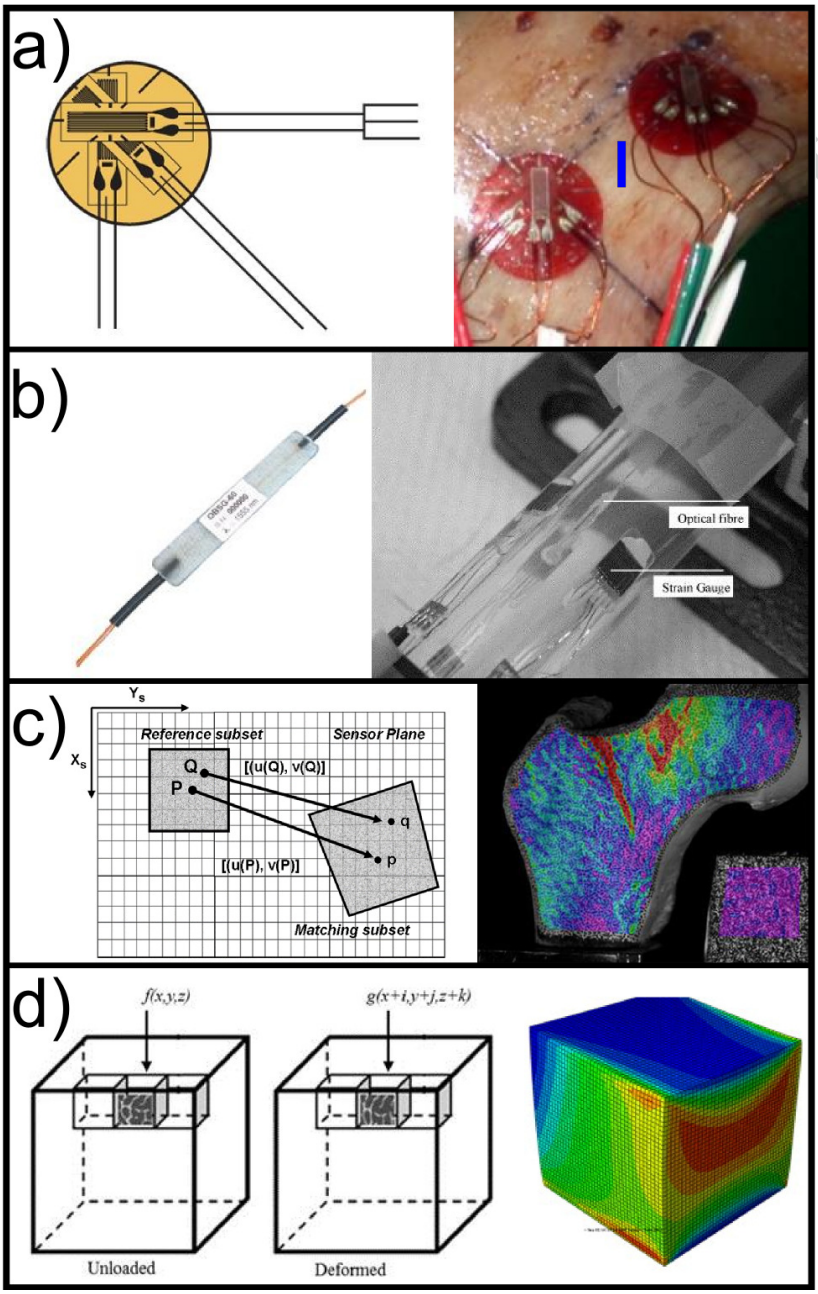

Highlights

- Review of strain measurement techniques with focus on bone experimental mechanics
- Strain gauges, fibre Bragg grating, digital image correlation, digital volume correlation
- Working principles, summary of main applications to bone mechanics, pros & cons